Disruption of the FMN-A524 interaction cascade and Glu513 induced collapse of the hydrophobic barrier promotes light induced Jα-helix unfolding in AsLOV2

Syeda Amna Arshi[1], Manisha Chauhan[1], Amit Sharma[1, 2]

[1]Multidisciplinary Centre for Advance Research and Studies, Jamia Millia Islamia, New Delhi, India

[2]**Author to whom correspondence should be addressed:**

Amit Sharma

Mailing address: Multidisciplinary Centre for Advance Research and Studies, Jamia Millia Islamia, Jamia Nagar New Delhi - 110025, India

Email: asharma4@jmi.ac.in

No. of manuscript pages: 23

No. of figures: 7

Description of Supplementary material

Filename: Suppl_AsLOV2

No. of supplementary material pages: 7

No. of supplementary figures: 6

ABSTRACT:

The C terminal Jα-helix of the *Avena Sativa's* Light Oxygen and Voltage (AsLOV2) protein, unfolds on exposure to blue light. This characteristic seeks relevance in applications related to engineering novel biological photoswitches. Using Molecular Dynamic (MD) simulations and the Markov State Modeling (MSM) approach we provide the mechanism that explains the stepwise unfolding of the Jα-helix. The unfolding was resolved into seven steps represented by the structurally distinguishable states distributed over the initiation and the post initiation phases. Wherein, the initiation phase occurs due to the collapse of the interaction cascade FMN-Q513-N492-L480-W491-Q479-V520-A524, the onset of the post initiation phase is marked by breaking of the hydrophobic interactions between the Jα-helix and the Iβ-sheet. This study indicates that the displacement of N492 out of the FMN binding pocket, not necessarily requiring Q513, is essential for the initiation of the Jα-helix unfolding. Rather, the structural reorientation of Q513 activates the protein to cross the hydrophobic barrier and enter the post initiation phase. Similarly, the structural deviations in N482, rather than its integral role in unfolding, could enhance the unfolding rates. Further, the MSM studies on the wild type and the Q513 mutant, provide the spatio-temporal roadmap that layout the possible pathways of structural transition between the dark and the light states of the protein. Overall, the study provides insights useful to enhance the performance of AsLOV2 based photoswitches.

Keywords: AsLOV2, Jα-helix, Molecular Dynamic (MD) simulations, Markov State Modeling (MSM), Stepwise unfolding, Initiation, Hydrophobic barrier, Spatio-temporal road map

Importance and/or impact of the work: As a light-sensitive protein, AsLOV2 has been widely demonstrated for its potential developing biological photoswitches. The mechanistic insights obtained from this study will be important to consider while designing novel and efficient photoswitches. Applications related to optogenetics and development of molecular tools in photobiology shall greatly benefit from this work.

INTRODUCTION:

Blue light receptors that are responsible for phototropism in plants (mainly angiosperms) also have a role in autophosphorylation[1], regulation of stomatal opening[2], chloroplast relocation[3,4] and leaf opening[5]. Light-Oxygen-Voltage (LOV) domain is one of the blue light receptors that belong to the Per-ARNT Sim (PAS) domain superfamily[6]. LOV domains are found in plants[7,8], bacteria[7,9], fungi[10–13] and algae[14,15]. These domains are instrumental in the development of artificial photoswitches that enable spatio-temporally precise regulation of the active and inactive states of the target proteins[16–25]. Light-Oxygen-Voltage domain of *Avena sativa* (AsLOV2) is being widely used in the development of these photoswitches such as the LINuS (regulates gene expression and entry to mitosis)[20], LEXY (control over the export proteins in cell)[23], LOV–TAP (regulates the TrpR binding to the DNA)[25] and BLISS (controls protein conjugation)[17].

AsLOV2 due to its small size, soluble nature and co-expression of its chromophore (FMN) makes this protein an ideal choice for designing photoswitches[26,27]. The core structure of AsLOV2 consists of 5 α-helices namely, an N terminal A'α (T407-R410), Cα (D432-T438), Dα (R442-E444), Eα (R451-L453) and Fα (R460-N472) and 5 β-sheets namely, Aβ (F415-T418), Bβ (I427-A430), Gβ (V476-Y483), Hβ (K489-R500) and Iβ (V506-G516) (PDB ID: 2V1A[28]). The protein's core at its C terminal is followed by the Jα-helix (D522-E545) that remains folded in dark. Whereas, in blue light (447 nm) the Jα-helix unfolds. This structural transition is a reversible process with timescales of unfolding and folding in microseconds and seconds, respectively[29]. This characteristic feature forms a basis for LOV2 to be used in photoswitching applications[16–25].

The FMN in the dark state remains noncovalently stabilized in the protein core through the set of H bonds between the FMN's (O2, N3, O4, O4) and the core's N482 (ND2), N482 (OD1), N492 (ND2) and Q513 (NE2), respectively. On exposure to light, photocycle initiates wherein, the singlet excited state of FMN undergoes intersystem crossing to the triplet excited state and subsequently leads to the formation of a covalent bond between FMN(C4A) and C450(SG) (Figure 1). This causes the protonation at the FMN(N5)[30] that flips the Q513 side chain that induces a formation of a H bond between FMN(N5) and Q513(OE1). While, other H bonds between the FMN and the atoms of N482 and N492 remain unaltered in the light crystal state (PDB ID: 2V1B[28,31]).

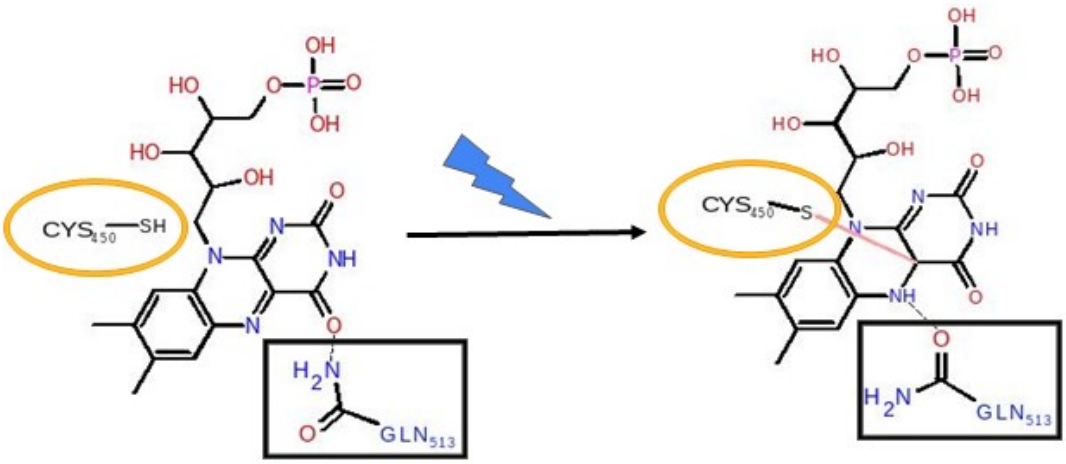

Figure 1: Blue light induced covalent bond (pink) between the thiol of C450 (yellow) and C4A carbon of FMN (black) flips Q513 side chain (rectangular black box)

Literature suggests that the residues from the AsLOV2 core regions, especially from the Iβ-sheet and A'α-helix play a crucial role in the light induced opening of the Jα-helix[32,33]. The study using a set of data collected from 5 independent dark and light induced Molecular Dynamic (MD) simulations of 200ns each suggested - the dynamics of Iβ-sheet and its conserved Q513 residue correlates with that of the Jα-helix[34]. Whereas a separate study based on MD simulations and other approaches like Markov state modeling, and machine learning, has suggested A'α-helix regulatory role in Jα-helix unfolding[35]. Furthermore, the MD study by Iuliano J N and team has demonstrated the complete unfolding of the AsLOV2 Jα-helix within 7 μs under the light conditions and provided a mechanistic insight suggesting that Q513 lever arm motion is essential for the Jα-helix unfolding[36]. Q513, for a long time, has been considered necessary for the stabilization of the light induced protonation at the N5 position of the FMN. And, its presence is pivotal for the development of the light induced cascade of structural changes that ultimately leads to unfolding[31–34]. In contrast, a recent study by Dietler *et al*., 2022, demonstrated that LOV photoreceptors remain functionally active irrespective of the presence of Q513[37]. In this work, the authors have reported successful, although sometimes attenuated, kinase activity for all the possible Q513 variants of the engineered AsLOV2 fused histidine kinase YF1, under the light conditions. Therefore, it's intriguing to understand the impact of Q513 on the molecular pathways that lead to light induced allostery in the Jα-helix.

Studying molecular pathways at atomic level, using experimental approaches have always been challenging. Alternatively, atomistic MD simulations have allowed to explore the allosteric changes in the biomolecules. In this study, we have captured the light-induced stepwise unfolding of the AsLOV2 Jα-helix and have identified its correlation with the secondary structural dynamics of the protein core. We explored the evolution of the structural attributes of the key residues involved in unfolding and their impact on the interaction linkage necessary for the stability of the Jα-helix. Using the data collected from various MD trajectories the Markov State Models (MSMs) were generated and the spatio-temporal pathways that lead to complete Jα-helix unfolding were analyzed. Lastly we explored the impact of Q513 on unfolding, by conducting studies on Q513 mutant.

RESULTS:

AsLOV2 Jα-helix unfolds in a stepwise manner

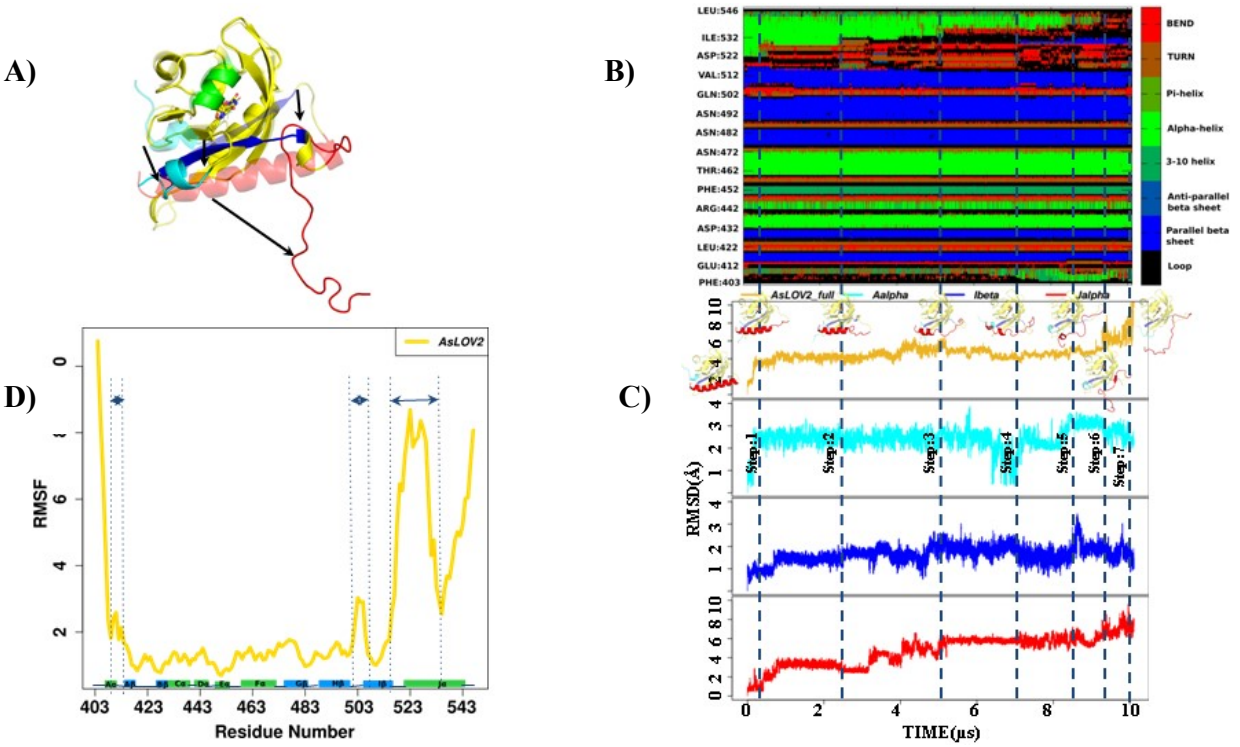

Figure 2: Overall secondary structural changes observed within the 10μs of FMN-CYS adduct formation. A) Structural comparison between the light structure with unfolded Jα-helix and the dark crystal structure (2V1A). The arrows indicate the changes from dark crystal structure to light structure. After 10μs Jα-helix (red) unfolds and moves away from the core (yellow) of the protein. While the core remains relatively stable, it's N-terminal Aα-helix (cyan) conformation changes to 3-10 helix and the Iβ-sheet (blue) shortens and bends away from the dark state position. B) DSSP map showing an evolution of the secondary structure over 10μs. C) Root Mean Square Deviation (RMSD) of the Cα atoms of the whole AsLOV2 (yellow), Aα-helix (cyan), Iβ-sheet (blue) and Jα-helix (red). Also, shown are the representative structures captured at different unfolding steps (dotted line) of the Jα-helix. D) Residue wise Root Mean Square Fluctuation (RMSF) of the Cα atoms of the AsLOV2. Regions with the high fluctuations are marked with in the vertical dotted lines.

The most prominent secondary structural change observed from the 10 μs MD simulation was the unfolding of AsLOV2's Jα-helix (Figure 2A). The residue-wise secondary structural projections of the Define Secondary Structure of Proteins (DSSP[38]) map (Figure 2B) showed that Jα-helix unfolding happens in a stepwise manner that synchronizes with the time dependent changes in the protein rmsd (Figure 2C). The first step after the light induction occurs at 0.7μs (Step 1). Until this point the Jα-helix unfolds between D522-G528. At 2.8 μs (Step2) the Jα-helix enters the second stage of unfolding, where residues G528-I532 begin to undergo a series of

transient conversions between the folded and the unfolded states. These interconversions lasts till 5.2μs (Step 3), beyond which the Jα-helix completely unfolds till I532 and the left over partition remains stably folded up to 7.0 μs (Step 4). Thereafter this partition switches into two helical structures between E537-D540 and A543-E545, in series. At 8.5μs (Step 5), these helical structures disappear and a single helical turn appears between I539-A543 which then vanishes by 9.3μs (Step 6). Finally, after an appearance of a short lived β-sheet between M529-I532, the Jα-helix unfolds completely to a loop at 10 μs (Step 7).

Localized dynamics in AsLOV2 core coordinates unfolding of the different segments of the Jα-helix

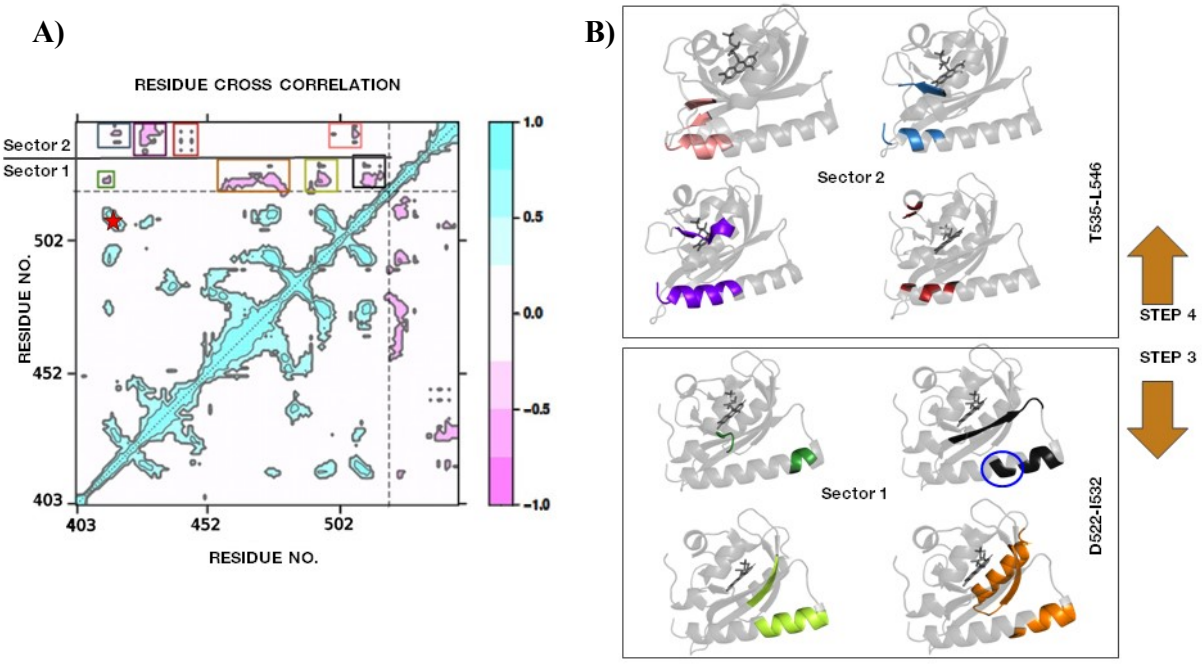

Figure 3: A) Dynamic cross correlation map (DCCM) of time-correlated backbone atom motions highlighting (colored boxes) correlated regions of the AsLOV2 Jα-helix with the core part of the protein. Highlighted regions are segregated into two sectors. B) Correlated regions corresponding to Sector 1 and Sector 2 are shown.

Shortening of Iβ-sheet and the transient conversion of A'α helix into the 3_{10}-helix and the loop were the next most pronounced influences observed, that light had on AsLOV2 (Figure 2A and 2B). The raised root mean square fluctuations seen in different regions of the core (Figure 2D) indicate, the light based conformational effects are not only limited to the A'α-helix and the Iβ-sheet. We investigated, using inter-residue dynamical cross-correlation matrix (DCCM) analysis, if these localized structural changes in the core coordinate with the stepwise Jα-helix unfolding? Overall, the dynamics between the residues of the Jα-helix and the core is prominently anti-correlated. Interesting to notice are the strongly ($|r| \geq 0.5$, where r is the correlation cutoff) cross-correlated regions (Figure 3A, colored boxes), distributed between two halves of the Jα-helix, the $J\alpha_N$ (the N-terminal half (D522-I532), Figure 3B Sector1) and the $J\alpha_C$ (the C-terminal half (T535-

L546), Figure 3B Sector2), separated by the un-correlated region ΔJα containing K533 and K534.

$J\alpha_N$ is negatively correlated to the three core regions, namely the Fα-helix to Gβ-sheet region (T458-N482, orange), the Hβ-sheet region (W491-P498, lime), and the Iβ-sheet along with its adjacent loop region (residue I510-E518, black). Noticeably, the respective regions contain the residues, N482, N492 and Q513, that mediate hydrogen bond linkages between the protein core and the FMN[36]. These residues are therefore the possible gateways to initiate the signaling for the Jα-helix unfolding. The significantly higher correlation estimates (-0.75) for the core region containing Q513 (black, Figure 3B) suggests, Q513 is a preferable gateway. It also seems favorable due to the dynamical correlation between the small loop region (K413-F415, green), located between the A'α-helix and the Aβ-sheet (Sector 1, Figure 3B), and the helical turn (A524-R526) in $J\alpha_N$. This loop region contains N414, which is essential for linking the Q513 dynamics to the Jα-helix unfolding[36]. The strong positive correlation (red star, Figure 3A) observed between Q513 containing Iβ-sheet (Figure 3B, black)and N414's loop (green) also emphasizes the strength of this linkage.

On the other hand, the $J\alpha_C$ houses four overlapping regions with the set of residues (I539, A542, A543, E545 and L546), (T535, A536, N538-L546), (A536, I539, D540, A543) and (I539-L546) which show strong correlation dynamics with the core regions, Aβ-sheet (V416-D419, blue), I427-F434 (purple), residues R442 and L446 (red), and the part of Hβ and the Iβ-sheet regions (499, 500, 507-509, pink), respectively.
These results indicate that the light induced structural changes in the specific core regions in the Sector 1 and Sector 2 (Figure 3B), could allosterically coordinate the unfolding of the $J\alpha_N$ and $J\alpha_C$ portions, respectively

Disruption of the interaction cascade linking the FMN and the Jα-helix N terminal is essential for the unfolding initiation

Q513, N492, N482 and N414 could regulate the initiation events of the Jα-helix unfolding. The time resolved structural analysis of these residues reveal how the Jα-helix unfolding initiates. It is observed that the FMN-CYS adduct lead protonation at the FMN(N5) triggers the movement of Q513 within 0.6μs (Figure 4). Wherein, N492 breaks its H bond contact with the FMN and forms a contact with Q513 (Figure 4 & Supp Figure 1d). At 0.7μs, Q513's backbone shifts downwards by 1.2 Å with respect to its dark state position and its side chain rotates by 116° out of the FMN binding pocket. This lever-like motion of Q513 pulls with it the N492, and disturbs N492's H bond interaction with N482 (Figure 4 & Supp Figure 1c). Simultaneously, L480 gets reoriented, which causes disruption in the series of vanderwaal interactions L480-W491-Q479 (Figure 5). This further triggers the breaking of H bond interaction between Q479 and V520. Q479 has been predicted to be important for Jα-helix stability[39]. The disruption cascade further breaks the H bond linkage between V520 and A524 (Jα-helix residue). V520-A524 linkage, in the dark state, is essential for the stability of the first helical turn of the Jα-helix[28]. Thus, disruption in the interaction linkage FMN-Q513-N492-L480-W491-Q479-V520-A524 is essential to initiate the Jα-helix unfolding.

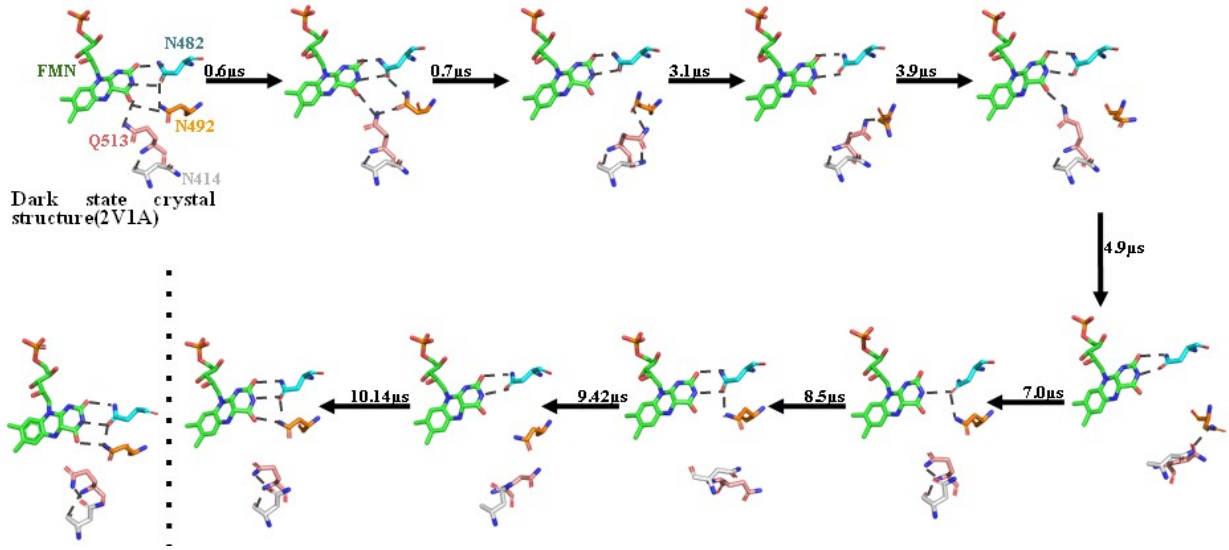

Figure 4: Residue wise conformational changes at the time intervals 0.6µs, 0.7µs, 3.1µs, 3.9µs, 4.9µs, 7.0µs, 8.5µs, 9.42µs and 10.14µs after the FMN-CYS bond formation. FMN, N482, N492, Q513 and N414 are shown as elements in green, cyan, orange and grey, respectively. H bonds are shown as black dotted lines. Residue wise structural orientations after 10.14µs compared with that of the light crystal state (2V1B).

N492's transient displacement, irrespective of Q513 suffice the initiation of the Jα-helix unfolding

A recent study by Dietler et al., 2022[37] suggested that unfolding of the Jα-helix is possible in the absence of Q513. To understand if the absence of Q513 impacts the interaction cascade leading to the initiation of the Jα-helix unfolding, we analyzed light based structural changes in AsLOV2 where Q513 was mutated to alanine (AsLOV2_Q513A) and to leucine (AsLOV2_Q513L). Although the complete unfolding was not observed in these mutants, they undergo the unfolding initiation (Figure 5D and 5F, Supp Figure 2). The initiation was marked by the similar secondary structural changes as in the case of the wild type protein. During initiation, both the mutants show transient movements of N492 out of the FMN binding pocket by breaking its H-bond interactions with FMN and N482 (Figure 5D, 5E, Supp Figure 3, 4). Like the wild type, mutants show disruption in the interaction cascade (FMN-N492-L480-W491-Q479-V520-A524) responsible for the onset of initiation. Further,we observed that in wild type soon after the N492's movement out of the FMN binding pocket N492 begins to set transient interactions with Q513 until 7µs (Figure 4). Thereafter, N492 returns to its conformations as in the dark and light state crystal structures. On the contrary, the study by Iuliano JN et al reported that N492 after leaving the FMN binding pocket, bridges a link between N482 and Q513 till 6.81µs and thereafter N492 losses all these interactions[36]. However, our observation suggests that for the Jα-helix unfolding to get initiated, even a transient displacement of N492 out of the FMN binding pocket is sufficient and can happen irrespective of the presence of Q513.

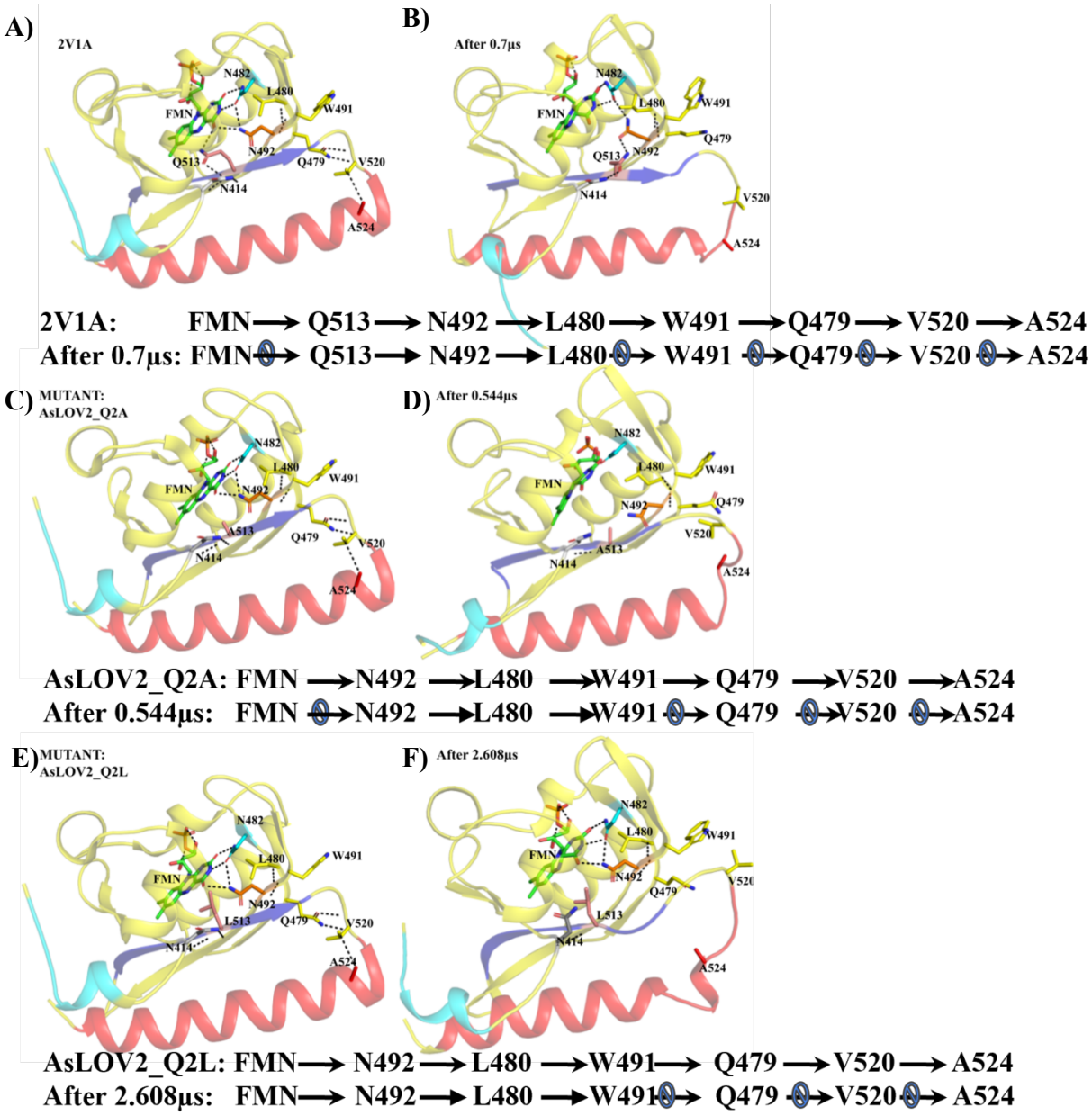

Figure 5: A), C) and E) Shown are the dark state structures of the wild type, AsLOV2_Q2A and AsLOV2_Q2L respectively and B), D) and F) Shown are the structures displaying unfolding initiation after 0.7, 0.54 and 2.7 µs and their corresponding interaction cascade between the FMN and the A524.

N482 dynamics could indirectly influence the rate of unfolding

Noticeably, N482 is not the part of the interaction cascade responsible for unfolding initiation. In contrast to the previous study[36], in our trajectories N482 never deviates from its dark state conformation (Figure 4 and Supp Figure 1 a, b). Also, the Jα-helix unfolding took 3µs longer to unfold (Figure 2B and 2C). These observations along with the fact that N482 shares the Gβ with

two of the interaction cascade residues L480 and Q479, any structural deviations in N482, could influence the rate at which Jα-helix unfolds.

Q513 reorientation promotes Jα-helix unfolding post initiation

We observed 0.7μs after the light induction Q513 moves out of the FMN binding pocket and thereafter does not form any interactions with FMN until 3.9μs. After which, Q513(NE2) possesses transient interactions with FMN(O4) until 4.9μs. Strikingly, this (4.9μs) time point just precedes Step 3, till which the Jα-helix transiently unfolds uptill I532 (Figure 2B and 2C). Also, at this time step, the Iβ-sheet further shortens until Q513 and drops further down by an angle of 11.2^{o} in comparison to its position at 3.9μs. This angular deviation corresponds to the 2Å shift in Q513 and its side chain reorients itself by 128.2^{o} (Figure 4). Similar positional changes around this time point have been observed previously[36]. Additionally, at 4.9μs we observed that Q513 loses its H bond contacts with N414 (Supp Figure 1I). These structural changes promote unfolding of the Jα-helix beyond I532. Further after 7.0μs Q513 side chain begins to flip by 180^{o}, which in concurrence with the complete unfolding the Jα-helix stabilizes in the orientation as found in the light state crystal structure. Maintaining its dynamical correlation with Q513, N414 also occupies the orientation as in the light crystal structure.

Spatio-temporal road map of AsLOV2 structural transition between its light induced states

Transition of AsLOV2 between its light induced states was studied through the Markov State Modelling (MSM)[40] approach on the cumulative 20 μs MD simulation data. Five metastable states were derived, where each state is a set of 10 markov models demonstrating the intra state structural variability (Figure 6). Occurrence probability of each state (represented by the size of the grey spheres) and the mean transition time between them (displayed on the connecting arrows) provided the spatio-temporal road map of transition from the fully folded (S2, blue) to the fully unfolded (S4, green) state of its Jα-helix. The transition happens via the set of intermediate states S3 (dark green), S1 (purple) and S5 (yellow).

Metastable states explain stepwise unfolding of the Jα-helix

Metastable State 2 (S2, blue): This is the second most occurring state (21.57%) with rmsd between the Cα atoms of the representative microstates 2.53±0.20 Å. Microstates in S2 correspond to the structural changes that happen within 0.7 μs (Figure 2C, Step1) of the light induction and are maximally occupied (80%) by the structure with the completely folded Jα-helix. S2 is stabilized due to the interactions as listed in Figure 6C, S2 box. Clearly, these interactions accommodate the initiation cascade FMN-Q513-N492-L480-W491-Q479-V520-A524 (Figure 6, S2 box, written in green). S2 is also occupied by a few microstates in which the Jα-helix remains partially folded until G528 and therefore resembles the structures on the verge of transition from completely folded Jα to unfolding initiation.

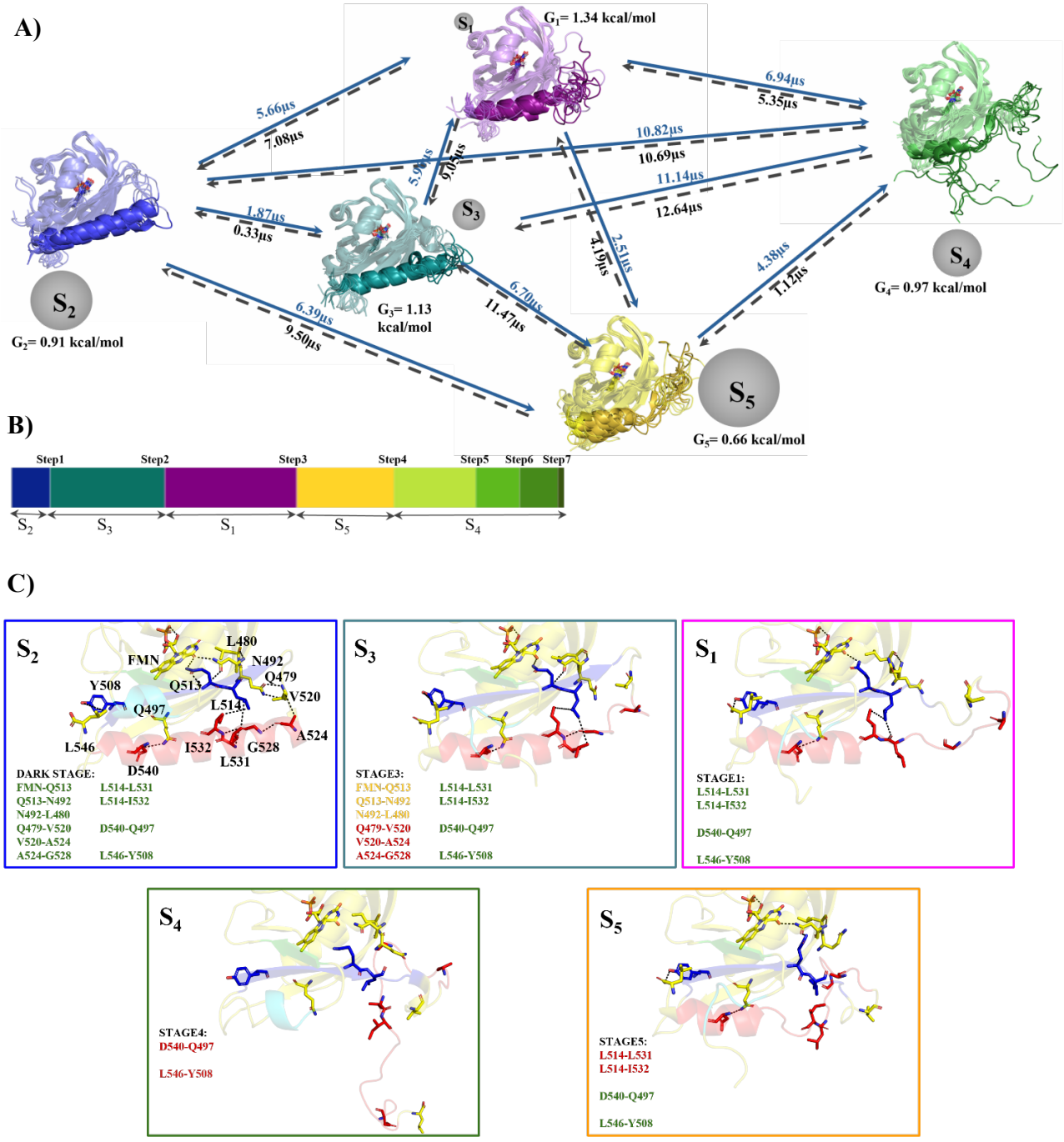

Figure 6: A) PCCA++ metastable states of wild type AsLOV2, along with mean first passage times (MFPTs) between them and their free energy. The size of the circles represents the occurrence probability of the particular state. B) Unfolding steps enveloped in the metastable states. C) Evolution of interactions in the metastable states. Represented are the persisting interactions (green), disturbed interactions (yellow) and lost interactions (red).

Metastable State 3 (S3, teal green): The probability of occurrence of this state is 15.05% with rmsd of 2.48±1.19Å. S3 is composed of the microstates with the Jα-helix unfolded up to G528 and accommodate structural changes between Step 1 and Step 2 (Figure 2C). This state possesses

the secondary structural changes that are considered as the signature of unfolding initiation. These structural changes seen in most of the microstates are (i) appearance of a small helical turn in the hinge region between the Iβ-sheet and the Jα-helix[35], (ii) appearance of the A'α-helix as 3_{10}-helix in 70% of the microstates, whereas 30% of these posses the A'α-helix region as a loop and (iii) the Iβ-sheet in S3 is found to be shorter by two residues and slightly bended towards Jα-helix. In S3, we observed that FMN-Q513-N492-L480 stretch of the interaction cascade gets disturbed (Figure 6, S3 box, written in yellow), whereas the linkage beyond L480, up till G528 gets completely shattered (Figure 6, S3 box, written in red).

Metastable State 1 (S1, magenta): This is the state with least occupancy (10.67%) with rmsd of 3.58±0.40Å. S1 comprises the microstates with the structural stages that lie between Step 2 (2.8 μs) and Step 3 (5.2 μs) of the simulation timeline (Figure 2C). Here, the A'α-helix remains completely unfolded and the majority of this metastable state possesses a shortened Iβ-sheet till L514. And, the structures contained in this state show the Jα-helix unfolding between G528 and I532. It is seen that the unfolding halts beyond I532, due to the hydrophobic interactions (L514-L531 and L514-I532) between the Iβ-sheet and the Jα-helix (Figure 6, S1 box).

Metastable State 5 (S5, yellow): S5 is the state with highest occupancy (32%) and has rmsd of 3.78±0.38Å. This metastable state comprises the structural stages of the Jα-helix between Step 3 (5.2 μs) and Step 4 (7.0 μs) (Figure 2C). In more than 70% of S5's microstate, Iβ-sheet further bends and shortens till Q513, which moves out of the FMN binding pocket and reorients by 180^{o}. This triggers L514, a residue adjacent to Q513, to lose its hydrophobic interactions (L514-L531 and L514-I532) with the Jα-helix (Figure 6, S5 box, written in red). As a result, the Jα-helix crosses this hydrophobic barrier and begins to unfold further beyond I532. Thereafter, due to the major H bond interactions that persist between the Jα's D540 and L546 with Hβ's Q497 and its adjacent loop residue Y508, respectively (Figure 6, S5 box, written in green), this state retains the unfolding of the Jα-helix only till I539.

Metastable State 4 (S4, green): S4 is majorly unfolded state that possesses 20% of the occupancy and highest structural deviation of 8.75±1.29Å. This state accommodates in it the markov state models that correspond to structures between Step 4 (7μs) to Step 7 (10.1μs) (Figure 2C). Here, 30% of the microstates retain a small helical turn between E541 and K544 residues of the unfolded Jα-helix. This feature sees an overlap with the structures found between Step 4 (7μs) and Step 6 (9.3 μs). The corresponding time window witnesses the breaking of the H bond between D540 and Q497. While, the loss of the last interaction (Y508-L546) appears in the remaining 70% of the metastable state and possesses markov models that correspond to the structures that appear after Step 6. In these microstates, the two-third population appears to contain a small stretch of a β sheet (in the Jα-helix) that corresponds to Step 6 to Step 7 (Figure 2C). Appearance of this β sheet is due to the H bond between T477 and M530. Whereas, in the remaining population, without this H bond, the Jα-helix remains completely unfolded as in the structures beyond Step7 (Figure 2C).

Q513 is pivotal for crossing the hydrophobic checkpoint

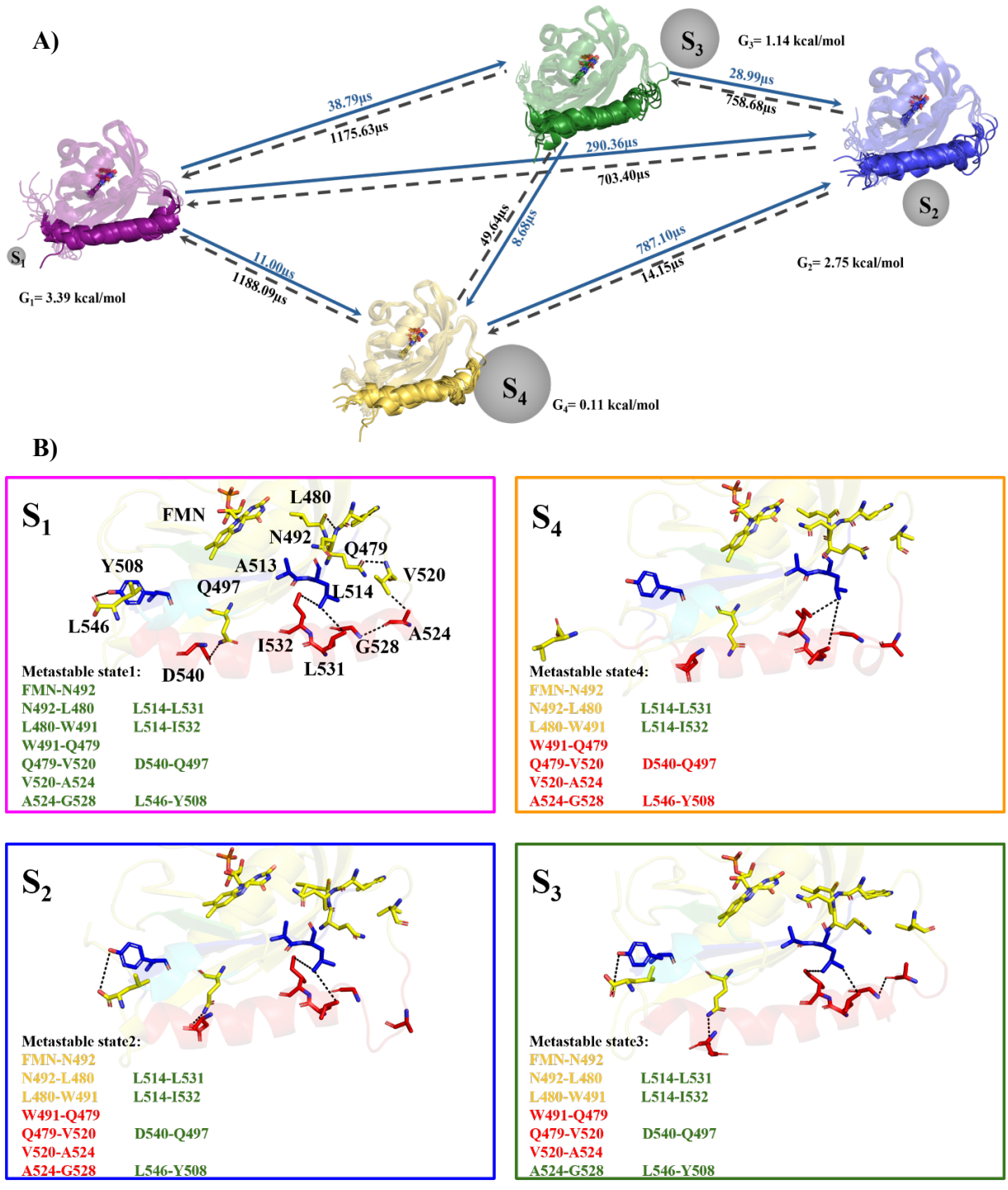

Figure 7: A) PCCA++ metastable states of mutated AsLOV2_Q513A, along with mean first passage times (MFPTs) between them and their free energy. The size of the circles represents the occurrence probability of the particular state. B) Residual network analysis of the 4 metatstable states representing the persisting interactions (green), disturbed interactions (yellow) and lost interactions (red).

The stepwise rupture of the Jα helix H bond interactions, necessary for its unfolding, halts at the site of hydrophobic interactions between the Iβ sheet and the Jα helix. Q513A and Q513L do not bypass this halt to resume the Jα-helix unfolding, at least 12 μs after the light induced state was created (Supp Figure 2). To understand the stringency of this hydrophobic checkpoint, we determined the markov state models of the Q513A mutant using the cumulative data of 24 μs MD simulations. Four metastable states S1, S2, S3 and S4 (Figure 7 and Supp Figure 6C) were obtained, of which the S1 holds microstates with the Jα-helix in a completely folded structural form. The representative models of the microstates in S1 (Figure 7, S1 box), shows that soon after the light induction in the Q513A mutant, the FMN loses its H-bond interactions with its active site residues. Thus, S1 is the least occupied (0.33%) state, and the mutant remains rather stable in the other states as their occurrences are 83%, 15% and 1%, in S4, S3 and S2 respectively. As presumed, due to the absence of Q513 all the metastable states possess intact hydrophobic bonds (L514-L531 and L514-I532) between the Iβ-sheet and the Jα-helix. Hence, the Jα-helix unfolding, in all the microstates, was found to be limited due to the hydrophobic checkpoint. S4 possessed unfolding between the E525 and E527, whereas in S3 and S2, unfolding could maximally extend until E527 and V529, respectively.

DISCUSSION:

Blue light absorption by AsLOV2 leads to Jα-helix unfolding[41]. Studies so far suggest, this allosteric characteristic is primed by the coordinated structural deviations such as unfolding of the A'α-helix, appearance of a helical turn between Iβ-sheet and Jα-helix, and loss of Iβ-sheet's N terminal stretch and its bending towards the Jα-helix[32,33,35,36]. Wherein, these deviations occur due to the changes in the structural attributes of the residues like Q513, N492, N482 and N414[36,39]. Specifically, Iuliano, J. N. *et al* proposed that Q513, through its structural reorientation and an interactive interplay with N414, establishes a signal transduction pathway between FMN and the Jα-helix to regulate unfolding[36].

In this study, using MD simulation and MSM approaches we have provided a detailed spatio-temporal journey of the light induced Jα-helix unfolding in AsLOV2. We explored the mechanistic contributions of the secondary structures and the residues that promote the Jα-helix unfolding at different stages. Starting from the N - terminal end the Jα-helix unfolds in seven time steps (Figure 2B & 2C). Further on the basis of the correlation dynamics between the Jα-helix and the AsLOV2 core these steps were segregated into two sectors, Sector 1 and Sector 2 (Figure 3). Sector 1 is composed (shown in orange, lime, black and green in Figure 3) of the core regions that correlates with the $J\alpha_N$ dynamics (D522 - I532) and corresponds with the unfolding time zone until Step 3 (5.2 μs). Sector 2 is the set of core regions (shown in red, purple, blue and pink in Figure 3) that correlates with the $J\alpha_C$ (T535 - L546) dynamics and corresponds to the time zone beyond Step 4 (7.0 μs). Interestingly, the region between $J\alpha_N$ and $J\alpha_C$, (ΔJα, K533 & K534) shows no dynamical correlation with the AsLOV2 core. And, the stable rmsd of the Jα-helix between Step 3 and Step 4 indicates its correspondence with the ΔJα.

The complete Jα-helix unfolding requires that the protein successfully unfolds through the two major stages, (i) entry point of the $J\alpha_N$ segment (initiation phase) and (ii) the ΔJα barrier. The Jα-

helix folded state is maintained via the interaction cascade (L480-W491-Q479-V520-A524) that links the FMN and the $J\alpha_N$ segment. Thus for unfolding initiation, it's essential to disrupt this cascade. Link between FMN and this cascade is mediated via Q513 and N492. But it was observed that even a momentary displacement of N492, out of the FMN binding pocket, irrespective of the presence of Q513, could cause the disruption in cascade (Figure 5). Additionally N482, like Q513 and N492, also forms the FMN binding pocket. But it does not show any direct linkage in the initiation cascade, although N482's structural dynamics could influence the rate of unfolding.

Secondly, to unfold through the ΔJα barrier, it is essential that the protein bypass a hydrophobic check point (L514-L531 and L514-I532) between the Iβ sheet and the Jα helix. It was observed, just beyond Step 3, Q513 reorients and triggers L514 which leads to breaking of its hydrophobic interactions before Step 4. Simultaneously, the A'α-helix (T407-R410) completely unfolds, which was otherwise undergoing the series of structural conversions between 3_{10}-helix and loop (Figure 2B). Until this point of time the A'α-helix shows minimal variations in its rmsd (Figure 2C). Thereafter, these variations enhance and their coordination with the changes in the Jα-helix rmsd become more pronounced. Previous studies have suggested that light induction in AsLOV2 causes deviations in the residues in the vicinity of the A'α helix[28,39]. Of these residues, N414 is of special importance due to its contribution in stabilizing the contacts between the A'α and the Jα-helix[42]. N414 is also critical due to its contribution in Jα-helix unfolding via the rearrangements in its interaction linkages with Q513[36]. Altogether these structural coordinations are suggestive of providing the necessary trigger required to push the Jα-helix into the unfolding state, cross the ΔJα barrier after a stint of stability between Step 3 and Step 4. To test this hypothesis, we analyzed light induced changes in AsLOV2 mutants which cease to attain Jα-helix unfolded state similar to that in the wild type at Step 4 (Figure 2). Unlike wild type, the complete unfolding of the A'α-helix (Supp Figure 2A and 2C) and the crossing of the hydrophobic checkpoint was not observed in Q513 mutants. Noticeably, the photosensors having these mutations are found to be functionally active, although with compromised efficiency[37]. Therefore, we suggest that in the absence of Q513, AsLOV2 could bypass the ΔJα barrier, but with delay. A recent finding supports this idea that Q513 mutants delays and not ceases, the AsLOV2 photocycle[43].

We found, in spite of the different spatio-temporal paths of Jα-helix unfolding, the structural attributes, that are specifically important to leap the protein through various unfolding stages, remain the same. These attributes are encompassed within the set of five metastable states (S1 to S5) estimated using the MSM approach. Overall, it was observed that the state with completely folded Jα-helix (Figure 6, S2) stabilizes the initiation cascade. With the loss of interactions in the initiation cascade, protein enters the initiation phase (Figure 6, S3). Then, the hydrophobic checkpoint halts the unfolding at the I532 residue of the Jα-helix (Figure 6, S1). Thereafter, due to the structural reorientation in Q513 the protein crosses the checkpoint (Figure 6, S5) and resumes complete unfolding (Figure 6, S4). Further on, the MSM studies on Q513A mutant suggested that, in spite of the coordinated layoff of the initiation cascade, inability of the mutant to bypass the hydrophobic checkpoint, in any of its metastable states, withheld the protein from complete unfolding.

Overall, the study provides the spatio-temporal roadmap for the light induced Jα-helix unfolding of AsLOV2. The structural insights discussed here are imperative and useful due to the central role of LOV2 in development of efficient photoswitches and it's applications like optogenetic[19,26], photobiology[12,14], photosynthesis[3] etc.

MATERIALS AND METHODS:

MD simulations:

MD simulations were performed as per the earlier study on AsLOV2[36] using Amber version 20[44].

Simulations conducted included a set of independent runs of 10 μs on AsLOV2, a set of two runs of 12 μs each of AsLOV2_Q513A and a set of one run of 12 μs on AsLOV2_Q513L. Starting structures used in all the cases was the modified dark crystal structure of AsLOV2 (PDB ID: 2V1A) in which the covalent bond was created between the C450-SH and FMN-C4A. Analysis was performed using Amber cpptraj[45], Bio3D[46] tool integrated into R (version 4.1.3[47]) and Pymol (version 2.3.0[48]).

Markov state modeling

pyEMMA (version 2.5.7[49]) was used to construct and analyze MSM. Detailed procedure used to conduct MSM study on 20 μs AsLOV2 and 24 μs AsLOV2_Q513A cumulative MD data is provided in the supplementary material section.

ACKNOWLEDGMENTS:

AS acknowledges the funding support from the UGC-FRP startup grant and DBT research grant No. BT/PR34567/10/1822/2019.

REFERENCES:

1. Christie, J. M., Reymond, P., Powell, G. K., Bernasconi, P., Raibekas, A. A., Liscum, E., & Briggs, W. R. (1998). Arabidopsis NPH1: A flavoprotein with the properties of a photoreceptor for phototropism. *Science (New York, N.Y.)*, *282*(5394), 1698–1701. https://doi.org/10.1126/science.282.5394.1698

2. Kinoshita, T., Doi, M., Suetsugu, N., Kagawa, T., Wada, M., & Shimazaki, K. (2001). Phot1 and phot2 mediate blue light regulation of stomatal opening. *Nature*, *414*(6864), 656–660. https://doi.org/10.1038/414656a

3. Sakai, T., Kagawa, T., Kasahara, M., Swartz, T. E., Christie, J. M., Briggs, W. R., Wada, M., & Okada, K. (2001). *Arabidopsis* nph1 and npl1: Blue light receptors that mediate both phototropism and chloroplast relocation. *Proceedings of the National Academy of Sciences*, *98*(12), 6969–6974. https://doi.org/10.1073/pnas.101137598

4. Sakamoto, K., & Briggs, W. R. (2002). Cellular and Subcellular Localization of Phototropin 1. *The Plant Cell*, *14*(8), 1723–1735. https://doi.org/10.1105/tpc.003293

5. Briggs, W. R., & Christie, J. M. (2002). Phototropins 1 and 2: Versatile plant blue-light receptors. *Trends in Plant Science*, *7*(5), 204–210. https://doi.org/10.1016/s1360-1385(02)02245-8

6. Taylor, B. L., & Zhulin, I. B. (1999). PAS domains: Internal sensors of oxygen, redox potential, and light. *Microbiology and Molecular Biology Reviews: MMBR*, *63*(2), 479–506. https://doi.org/10.1128/MMBR.63.2.479-506.1999

7. Crosson, S., & Moffat, K. (2002). Photoexcited structure of a plant photoreceptor domain reveals a light-driven molecular switch. *The Plant Cell*, *14*(5), 1067–1075. https://doi.org/10.1105/tpc.010475

8. Somers, D. E., Schultz, T. F., Milnamow, M., & Kay, S. A. (2000). ZEITLUPE encodes a novel clock-associated PAS protein from Arabidopsis. *Cell*, *101*(3), 319–329. https://doi.org/10.1016/s0092-8674(00)80841-7

9. Losi, A., Polverini, E., Quest, B., & Gärtner, W. (2002). First evidence for phototropin-related blue-light receptors in prokaryotes. *Biophysical Journal*, *82*(5), 2627–2634. https://doi.org/10.1016/S0006-3495(02)75604-X

10. Froehlich, A. C., Liu, Y., Loros, J. J., & Dunlap, J. C. (2002). White Collar-1, a circadian blue light photoreceptor, binding to the frequency promoter. *Science (New York, N.Y.)*, *297*(5582), 815–819. https://doi.org/10.1126/science.1073681

11. Heintzen, C., Loros, J. J., & Dunlap, J. C. (2001). The PAS protein VIVID defines a clock-associated feedback loop that represses light input, modulates gating, and regulates clock resetting. *Cell*, *104*(3), 453–464. https://doi.org/10.1016/s0092-8674(01)00232-x

12. Idnurm, A., & Heitman, J. (2005). Light Controls Growth and Development via a Conserved Pathway in the Fungal Kingdom. *PLOS Biology*, *3*(4), e95. https://doi.org/10.1371/journal.pbio.0030095

13. Schwerdtfeger, C., & Linden, H. (2001). Blue light adaptation and desensitization of light signal transduction in Neurospora crassa. *Molecular Microbiology*, *39*(4), 1080–1087. https://doi.org/10.1046/j.1365-2958.2001.02306.x

14. Takahashi, F., Yamagata, D., Ishikawa, M., Fukamatsu, Y., Ogura, Y., Kasahara, M., Kiyosue, T., Kikuyama, M., Wada, M., & Kataoka, H. (2007). AUREOCHROME, a photoreceptor required for photomorphogenesis in stramenopiles. *Proceedings of the National Academy of Sciences*, *104*(49), 19625–19630. https://doi.org/10.1073/pnas.0707692104

15. Henry, L., Berntsson, O., Panman, M. R., Cellini, A., Hughes, A. J., Kosheleva, I., Henning, R., & Westenhoff, S. (2020). New Light on the Mechanism of Phototransduction in Phototropin. *Biochemistry*, *59*(35), 3206–3215. https://doi.org/10.1021/acs.biochem.0c00324

16. Ahmad, T., Vullhorst, D., Chaudhuri, R., Guardia, C. M., Chaudhary, N., Karavanova, I., Bonifacino, J. S., & Buonanno, A. (2022). Transcytosis and trans-synaptic retention by postsynaptic ErbB4 underlie axonal accumulation of NRG3. *Journal of Cell Biology*, *221*(7), e202110167. https://doi.org/10.1083/jcb.202110167

17. Gil, A. A., Carrasco-López, C., Zhu, L., Zhao, E. M., Ravindran, P. T., Wilson, M. Z., Goglia, A. G., Avalos, J. L., & Toettcher, J. E. (2020). Optogenetic control of protein binding using light-switchable nanobodies. *Nature Communications*, *11*(1), Article 1. https://doi.org/10.1038/s41467-020-17836-8

18. Hartzell, E. J., Terr, J., & Chen, W. (2021). Engineering a Blue Light Inducible SpyTag System (BLISS). *Journal of the American Chemical Society*, *143*(23), 8572–8577. https://doi.org/10.1021/jacs.1c03198

19. Losi, A., Gardner, K. H., & Möglich, A. (2018). Blue-Light Receptors for Optogenetics. *Chemical Reviews*, *118*(21), 10659–10709. https://doi.org/10.1021/acs.chemrev.8b00163

20. Lungu, O. I., Hallett, R. A., Choi, E. J., Aiken, M. J., Hahn, K. M., & Kuhlman, B. (2012). Designing photoswitchable peptides using the AsLOV2 domain. *Chemistry & Biology*, *19*(4), 507–517. https://doi.org/10.1016/j.chembiol.2012.02.006

21. Niopek, D., Benzinger, D., Roensch, J., Draebing, T., Wehler, P., Eils, R., & Di Ventura, B. (2014). Engineering light-inducible nuclear localization signals for precise spatiotemporal control of protein dynamics in living cells. *Nature Communications*, *5*, 4404. https://doi.org/10.1038/ncomms5404

22. Niopek, D., Wehler, P., Roensch, J., Eils, R., & Di Ventura, B. (2016). Optogenetic control of nuclear protein export. *Nature Communications*, *7*(1), Article 1. https://doi.org/10.1038/ncomms10624

23. Polstein, L. R., & Gersbach, C. A. (2012). Light-inducible spatiotemporal control of gene activation by customizable zinc finger transcription factors. *Journal of the American Chemical Society*, *134*(40), 16480–16483. https://doi.org/10.1021/ja3065667

24. Strickland, D., Moffat, K., & Sosnick, T. R. (2008). Light-activated DNA binding in a designed allosteric protein. *Proceedings of the National Academy of Sciences*, *105*(31), 10709–10714. https://doi.org/10.1073/pnas.0709610105

25. Zoltowski, B. D., Motta-Mena, L. B., & Gardner, K. H. (2013). Blue light-induced dimerization of a bacterial LOV-HTH DNA-binding protein. *Biochemistry*, *52*(38), 6653–6661. https://doi.org/10.1021/bi401040m

26. Christie, J. M., Gawthorne, J., Young, G., Fraser, N. J., & Roe, A. J. (2012). LOV to BLUF: Flavoprotein contributions to the optogenetic toolkit. *Molecular Plant*, *5*(3), 533–544. https://doi.org/10.1093/mp/sss020

27. Shcherbakova, D. M., Shemetov, A. A., Kaberniuk, A. A., & Verkhusha, V. V. (2015). Natural photoreceptors as a source of fluorescent proteins, biosensors, and optogenetic tools.

Annual Review of Biochemistry, *84*, 519–550. https://doi.org/10.1146/annurev-biochem-060614-034411

28. Halavaty, A. S., & Moffat, K. (2007). N- and C-terminal flanking regions modulate light-induced signal transduction in the LOV2 domain of the blue light sensor phototropin 1 from Avena sativa. *Biochemistry*, *46*(49), 14001–14009. https://doi.org/10.1021/bi701543e
29. Kennis, J. T. M., Crosson, S., Gauden, M., van Stokkum, I. H. M., Moffat, K., & van Grondelle, R. (2003). Primary reactions of the LOV2 domain of phototropin, a plant blue-light photoreceptor. *Biochemistry*, *42*(12), 3385–3392. https://doi.org/10.1021/bi034022k
30. Yee, E. F., Diensthuber, R. P., Vaidya, A. T., Borbat, P. P., Engelhard, C., Freed, J. H., Bittl, R., Möglich, A., & Crane, B. R. (2015). Signal transduction in light–oxygen–voltage receptors lacking the adduct-forming cysteine residue. *Nature Communications*, *6*(1), Article 1. https://doi.org/10.1038/ncomms10079
31. Harper, S. M., Neil, L. C., & Gardner, K. H. (2003). Structural basis of a phototropin light switch. *Science (New York, N.Y.)*, *301*(5639), 1541–1544. https://doi.org/10.1126/science.1086810
32. Nash, A. I., Ko, W.-H., Harper, S. M., & Gardner, K. H. (2008). A conserved glutamine plays a central role in LOV domain signal transmission and duration. *Biochemistry*, *47*(52), 13842–13849. https://doi.org/10.1021/bi801430e
33. Nozaki, D., Iwata, T., Ishikawa, T., Todo, T., Tokutomi, S., & Kandori, H. (2004). Role of Gln1029 in the photoactivation processes of the LOV2 domain in adiantum phytochrome3. *Biochemistry*, *43*(26), 8373–8379. https://doi.org/10.1021/bi0494727
34. Freddolino, P. L., Gardner, K. H., & Schulten, K. (2013). Signaling mechanisms of LOV domains: New insights from molecular dynamics studies. *Photochemical & Photobiological Sciences: Official Journal of the European Photochemistry Association and the European Society for Photobiology*, *12*(7), 1158–1170. https://doi.org/10.1039/c3pp25400c

35. Ibrahim, M. T., Trozzi, F., & Tao, P. (2022). Dynamics of hydrogen bonds in the secondary structures of allosteric protein Avena Sativa phototropin 1. *Computational and Structural Biotechnology Journal*, *20*, 50–64. https://doi.org/10.1016/j.csbj.2021.11.038

36. Iuliano, J. N., Collado, J. T., Gil, A. A., Ravindran, P. T., Lukacs, A., Shin, S., Woroniecka, H. A., Adamczyk, K., Aramini, J. M., Edupuganti, U. R., Hall, C. R., Greetham, G. M., Sazanovich, I. V., Clark, I. P., Daryaee, T., Toettcher, J. E., French, J. B., Gardner, K. H., Simmerling, C. L., … Tonge, P. J. (2020). Unraveling the Mechanism of a LOV Domain Optogenetic Sensor: A Glutamine Lever Induces Unfolding of the Jα Helix. *ACS Chemical Biology*, *15*(10), 2752–2765. https://doi.org/10.1021/acschembio.0c00543

37. Dietler, J., Gelfert, R., Kaiser, J., Borin, V., Renzl, C., Pilsl, S., Ranzani, A. T., García de Fuentes, A., Gleichmann, T., Diensthuber, R. P., Weyand, M., Mayer, G., Schapiro, I., & Möglich, A. (2022). Signal transduction in light-oxygen-voltage receptors lacking the active-site glutamine. *Nature Communications*, *13*(1), Article 1. https://doi.org/10.1038/s41467-022-30252-4

38. Kabsch, W., & Sander, C. (1983). Dictionary of protein secondary structure: Pattern recognition of hydrogen-bonded and geometrical features. *Biopolymers*, *22*(12), 2577–2637. https://doi.org/10.1002/bip.360221211

39. Zayner, J. P., Antoniou, C., & Sosnick, T. R. (2012). The amino-terminal helix modulates light-activated conformational changes in AsLOV2. *Journal of Molecular Biology*, *419*(1–2), 61–74. https://doi.org/10.1016/j.jmb.2012.02.037

40. Malmstrom, R. D., Lee, C. T., Van Wart, A. T., & Amaro, R. E. (2014). Application of Molecular-Dynamics Based Markov State Models to Functional Proteins. *Journal of Chemical Theory and Computation*, *10*(7), 2648–2657. https://doi.org/10.1021/ct5002363

41. Konold, P. E., Mathes, T., Weiβenborn, J., Groot, M. L., Hegemann, P., & Kennis, J. T. M. (2016). Unfolding of the C-Terminal Jα Helix in the LOV2 Photoreceptor Domain

Observed by Time-Resolved Vibrational Spectroscopy. *The Journal of Physical Chemistry Letters*, *7*(17), 3472–3476. https://doi.org/10.1021/acs.jpclett.6b01484

42. Zayner, J. P., Mathes, T., Sosnick, T. R., & Kennis, J. T. M. (2019). Helical Contributions Mediate Light-Activated Conformational Change in the LOV2 Domain of Avena sativa Phototropin 1. *ACS Omega*, *4*(1), 1238–1243. https://doi.org/10.1021/acsomega.8b02872
43. Maity, S., Price, B. D., Wilson, C. B., Mukherjee, A., Starck, M., Parker, D., Wilson, M. Z., Lovett, J. E., Han, S., & Sherwin, M. S. (2023). Triggered Functional Dynamics of AsLOV2 by Time-Resolved Electron Paramagnetic Resonance at High Magnetic Fields. *Angewandte Chemie (International Ed. in English)*, *62*(13), e202212832. https://doi.org/10.1002/anie.202212832
44. Case, D. A., Cheatham, T. E., Darden, T., Gohlke, H., Luo, R., Merz, K. M., Onufriev, A., Simmerling, C., Wang, B., & Woods, R. J. (2005). The Amber biomolecular simulation programs. *Journal of Computational Chemistry*, *26*(16), 1668–1688. https://doi.org/10.1002/jcc.20290
45. Roe, D. R., & Cheatham, T. E. (2013). PTRAJ and CPPTRAJ: Software for Processing and Analysis of Molecular Dynamics Trajectory Data. *Journal of Chemical Theory and Computation*, *9*(7), 3084–3095. https://doi.org/10.1021/ct400341p
46. Grant, B. J., Rodrigues, A. P. C., ElSawy, K. M., McCammon, J. A., & Caves, L. S. D. (2006). Bio3d: An R package for the comparative analysis of protein structures. *Bioinformatics*, *22*(21), 2695–2696. https://doi.org/10.1093/bioinformatics/btl461
47. {R Core Team}. (2022). R: A language and environment for statistical computing. *R Foundation for Statistical Computing, Vienna, Austria.* https://www.R-project.org/
48. Schrödinger, LLC. (2015). *The PyMOL Molecular Graphics System, Version 2.3*.
49. Scherer, M. K., Trendelkamp-Schroer, B., Paul, F., Pérez-Hernández, G., Hoffmann, M., Plattner, N., Wehmeyer, C., Prinz, J.-H., & Noé, F. (2015). PyEMMA 2: A Software

Package for Estimation, Validation, and Analysis of Markov Models. *Journal of Chemical Theory and Computation*, *11*(11), 5525–5542. https://doi.org/10.1021/acs.jctc.5b00743